Proceedings Paper:

Allanic, R., Le Berre, D., Quendo, C. et al. (5 more authors) (2023) Monolithic frequency-reconfigurable antenna on silicon carbide for constrained environments. In: 2023 IEEE Conference on Antenna Measurements and Applications (CAMA). 2023 IEEE Conference on Antenna Measurements and Applications (CAMA), 15-17 Nov 2023, Genoa, Italy. Institute of Electrical and Electronics Engineers (IEEE) , pp. 649-652. ISBN 9798350323054

https://doi.org/10.1109/cama57522.2023.10352802

Monolithic Frequency-Reconfigurable Antenna on Silicon Carbide for Constrained Environments

Rozenn Allanic[1], Denis Le Berre[1], Cédric Quendo[1]
Univ. Brest, Lab-STICC
CNRS, UMR 6285
Brest, France
Rozenn.Allanic@univ-brest.fr

Edward A Ball[2], Jo Shien Ng[2], Guanwei Huang[2]
The University of Sheffield, Dept of Electronic & Electrical Engineering
Sheffield, UK
j.s.ng@sheffield.ac.uk

Aude Leuliet[3], Thomas Merlet[3]
Thales LAS OME
Élancourt, France
thomas.merlet@thalesgroup.com

***Abstract*— The paper presents a frequency reconfigurable bowtie antenna designed on silicon carbide (SiC) substrate. A monolithic active antenna is achieved thanks to the co-design method between the active integrated junctions and the bowtie antenna. Indeed, the semiconductor substrate allows doping distributed areas to obtain integrated N^+P^+ junction into the substrate co-designed in a same process flow as the antenna. When the junctions are forward biased, they connect a pair of stubs to the antenna creating a second resonant frequency. The global co-design approach offers possibilities to optimize the antenna in both frequencies. In the prototype, the resonant frequency can be switched from 20.5 GHz to 17.3 GHz.**

Keywords*— *Antenna, bowtie, frequency, reconfigurable, silicon carbide (SiC), ScDDAs, tunable.

I. Introduction

Nowadays, smart systems are omnipresent and antenna designers must face many constraints to meet a system's operating requirements, namely: low cost, high level of integration for size reduction, increased performance, and sometimes operation in harsh environments. Bowtie antennas are good candidate solutions for their ease of manufacture [1]-[4], with frequency agility possible using vanadium dioxide [5], or PIN diodes [6]- [7]. Adding active components such as surface-mounted devices (SMDs) can cause parasitic effects. Indeed, these SMDs are often small compared with the microstrip lines inducing mismatching and losses. One solution is to co-design and to fabricate the active elements and passive components in the same processes. A co-design method was previously proposed for a resonator and two distributed doped areas [8]. This offers a great flexibility in the choice of size and position of the doped areas. Moreover, a silicon carbide (SiC) substrate [9] with high permittivity increases compactness and gives an answer to high constraints environments with a high-level of power handling and temperature capability. Taking into account the co-design method, the idea in this work is to make a reconfigurable antenna on a SiC substrate.

Taking advantage of the co-design flexibility, this paper implements a bowtie antenna that is designed with two stubs connected to the antenna with distributed doped areas allowing the frequency reconfigurability. This antenna is designed on 4H-SiC to offer solution in compactness and performances in constrained environments. Therefore, Section II explains the idea and proposes the antenna design. Then, Section III details the simulations procedure and the simulated results. The fabrication process is described in Section IV followed by the measurement setup and the measured results in Section V. Finally, Section VI discusses the perspectives of this work.

II. Antenna Design

Figure 1 shows the frequency reconfigurable antenna. This is a bowtie antenna with a pair of stubs on a 4H-SiC substrate. Since it is a semiconductor substrate, co-design of the passive component and the active elements at the same time and in the same process flow was carried out. Two integrated junctions (in red in Fig. 1 (a)) in the substrate formed by a P^+ doped area (in blue in Fig. 1 (b)) and an N^+ doped area (in green) either isolate (OFF-state) or connect (ON-state) a pair of stubs. Figure 2 (a) shows a side view of a part of the antenna to zoom in one integrated junction. Figures 2 (b) and (c) illustrate the simplified models, respectively when the junction is not biased in the OFF-state and when the junction is direct biased in the ON-state. This additional pair of stubs increases the electrical length of the antenna when the stubs are connected to the bowtie antenna, thus offering a shift in the resonant frequency to the low frequency.

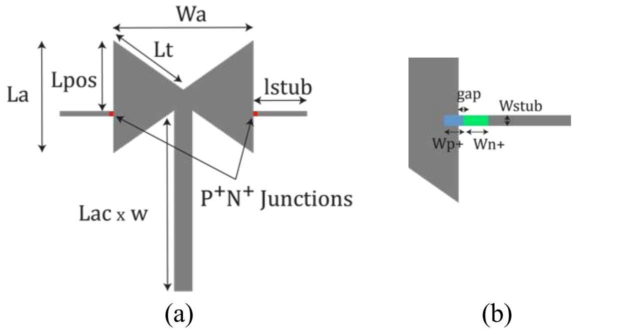

Fig. 1 Bowtie antenna with integrated junctions (a) Top view. (b) Side view.

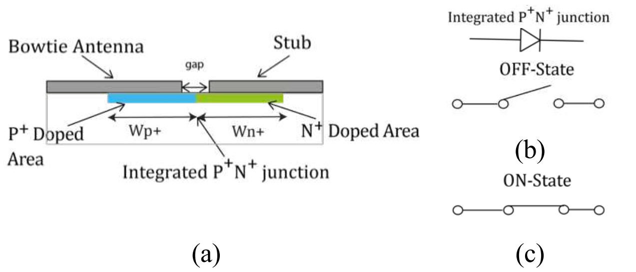

Fig. 2. (a) Side view of the antenna, zoom on the integrated junction. (b) OFF-state simplified model of the junction. (c) ON-state simplified model of the junction.

III. Simulated Results

The electromagnetic behavior of this reconfigurable antenna is simulated using HFSS™ from Ansys©. The dielectric permittivity of the 4H-SiC substrate is fixed at 9.7. As a first approximation the junctions are not simulated in the OFF-state and replaced by aluminum contacts in the ON-state. The antenna was designed to first resonates around 20 GHz. Therefore, with the dimensions given in Table 1, the simulated results are presented in Fig. 3. They show a resonant frequency in the OFF-state at 20.8 GHz with a 6.1 dB realized gain whereas in the ON-state the resonant frequency is at 17.3 GHz with a 3.1 dB realized gain, due to the dimensions of the stubs. Table 2 sums up the simulated antenna performances in both-states.

Table 1. Dimensions in mm of the bowtie antenna

Wa	La	Lpos	Lt	Lt	Lac	Wac
3.6	2.9	1.2	2.2	2.2	4.65	0.47
Lstub	Wstub	gap	Wp+	Wn+		
1.52	0.128	0.02	0.2	0.2		

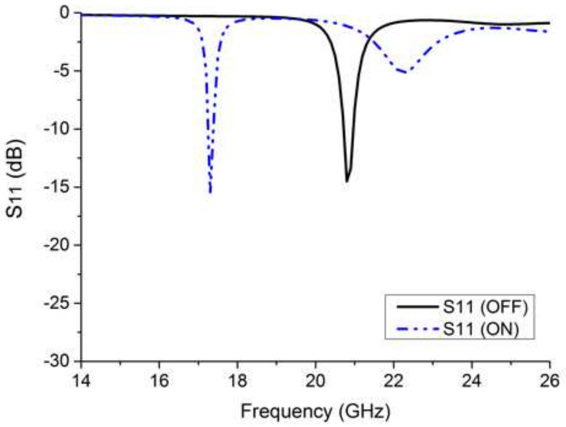

(a)

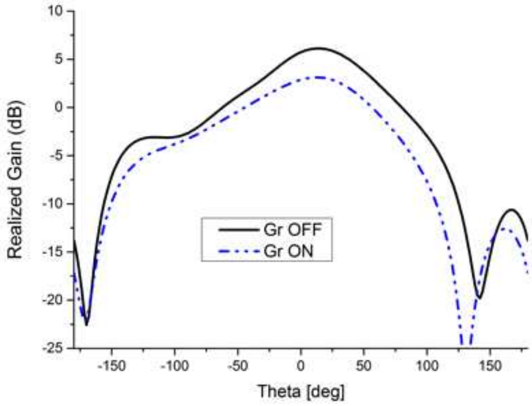

(b)

Fig. 3. Simulated results of the antenna. (a) S_{11}. (b) Realized Gain.

Table 2. Antenna simulated performances in both-states.

	Frequency	S11	Realized Gain
OFF-State	20.8 (GHz)	-15 (dB)	6.1 (dB)
ON-state	17.3 (GHz)	-15 (dB)	3.1 (dB)

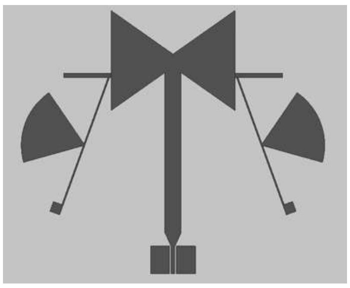

(a)

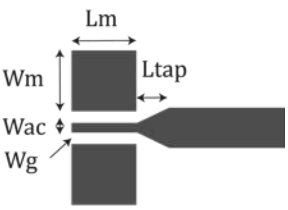

(b)

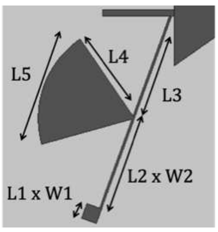

(c)

Fig. 4. (a) Antenna design. (b) zoom on the coplanar access. (c) zoom on the polarization circuit.

Table 3. Dimensions in mm of coplanar access and the bias circuit

Wm	Lm	Ltap	Wac	Wg		
0.55	0.8	0.39	0.114	0.044		
L1	W1	L2	W2	L3	L4	L5
0.3	0.3	1.85	0.04	2.07	1.8	2.14

A coplanar transition and a bias circuit were added to the antenna, such as in Fig. 4, to enable easy measurement with a probe station and to be able to bias the integrated junction minimizing the disturbances. Their dimensions are given in Table 3.

IV. Fabrication

The manufacture was done on a 350-µm thick 4H-SiC semi-insulating substrate. The process steps are summed up in Fig 5. Five masks are required for alignment marks, implantation of p (Boron) and n (Nitrogen), dielectric opening and top metal contact.

The fabrication process started with creating an alignment mark which then were dry etched into the substrate. Since relatively high implant energy was chosen, a 1-µm SiO2 was deposited as pattering oxide to protect the undoped area instead of normal photoresist for both p and n implantation. After patterning the doped area, the patterning oxide was dry etched to the substrate followed by a 30 nm screening oxide deposition. Both implanted target depth for p and n is 500 nm with doping concentration higher than 1E+18 cm^{-3}. It was observed that the color of the implanted area became dark due to the crystal damage from implantation, and then it was removed by rapid thermal annealing at a very high temperature (>1400°C). A 600 nm fresh oxide was deposited and then the doped area was opened by standard photolithography with the dielectric opening mask. Finally, metal Ti/Au with a thickness of 40/400 nm was deposited on the top and bottom of the substrate without further annealing.

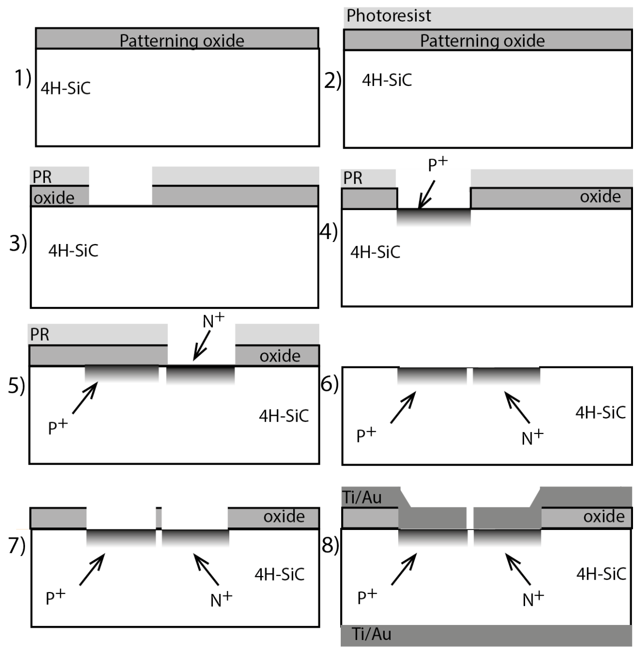

Fig. 5. Process steps

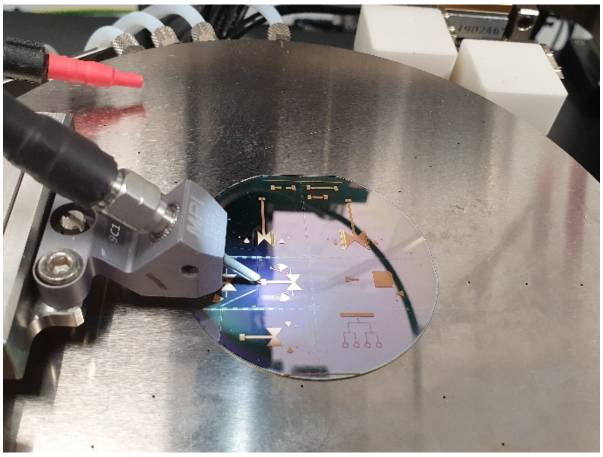

Fig. 6. Fabricated antenna on main probe station [10].

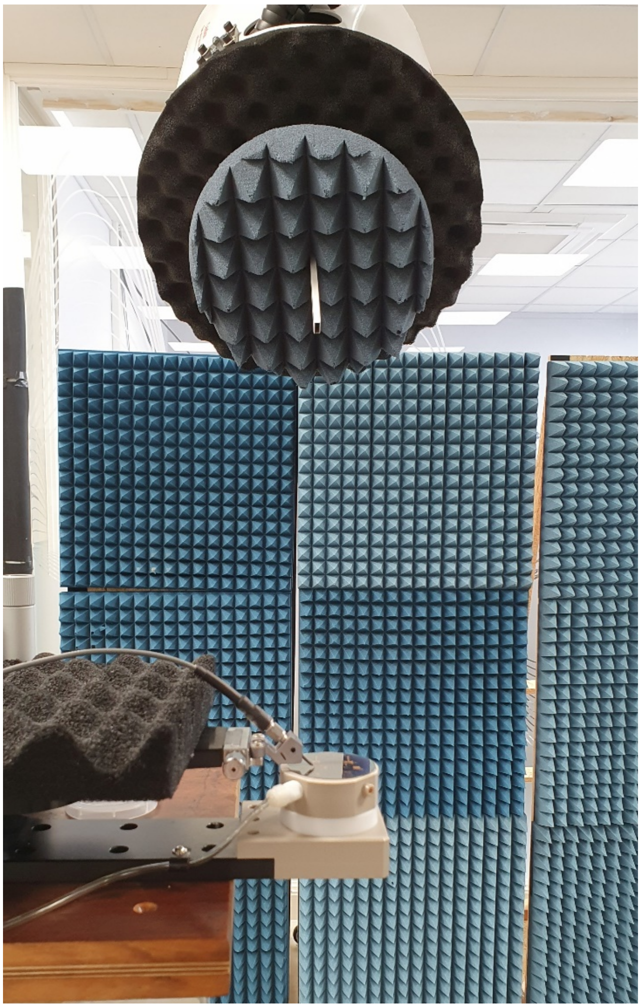

Fig. 7. Antenna undergoing radiated test on special mini prober station (phi sweep is vertically downwards as viewed here) [10].

V. Measured Results

Figure 6 shows the fabricated antenna on main probe station. Tests were jointly performed at the University of Brest and at the UKRI National mmWave Measurement Laboratory [10] at the University of Sheffield. Figure 7 illustrates the antenna undergoing radiated test on special mini prober station (phi sweep is vertically downwards).

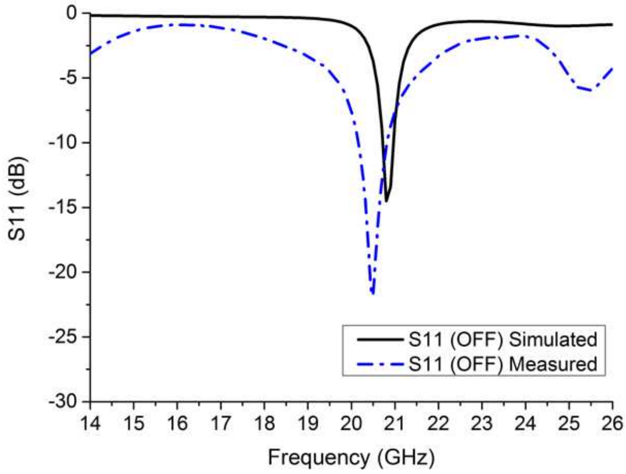

Fig. 8. Comparison between S11 simulated and measured results.

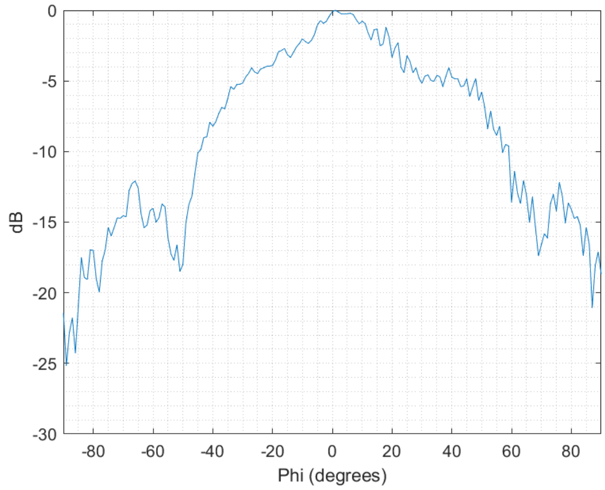

Fig. 9. Normalized Measured Radiation Pattern at location of peak power (diodes unbiased).

Unfortunately, the process steps were not able to achieve quantity of doping atoms as high as required. This implies that the integrated junction is not working in the ON-state, and the measured results are only presented in their OFF-state. To measure the demonstrator behavior, it was firstly placed on a probe station where a 67A-GSG-150-DP probe was used to measure the reflection coefficient with a vector network analyzer (VNA) ZVA67 from Rhodes & Schwarz. Figure 8 compares the simulated and measured results of the reflection coefficient. The measured resonant frequency is at 20.5 GHz and the reflection coefficient is -22 dB at the resonant frequency.

The wafer probes affect the gain measurements for certain radiated cuts, so Fig. 9 shows the results of phi cut at theta position of maximum gain. The maximum gain measured was +7.4 dBi.

VI. Conclusion

The monolithic frequency reconfigurable bowtie antenna presented in this paper aims to achieve low-cost, high integration level and ablility to work in highly constraint driven environments. Despite the process steps not allowing the frequency commutation, the concept is promising and the measured results show good performances in the OFF-state.

ACKNOWLEDGMENT

The authors would like to thank both governmental agencies in UK and France, namely DSTL and DGA, for their financial support operated in the frame of the MCM ITP (Material & Components for Missiles, Innovation Technology Partnership). The authors also would like to thank the TECHYP platform (the High Performance Computing Cluster at Lab-STICC) thanks to which the devices could be simulated. The authors would like to thank Steve Marsden, Dr. Sumin David Joseph and Sideqe Askre for wafer testing at the EPSRC National mmWave Measurement Lab.

REFERENCES

[1] H. Liu, H. Jiang, X. Guan, J. Lei and S. Li, "Single-Feed Slotted Bowtie Antenna for Triband Applications," in *IEEE Antennas and Wireless Propagation Letters*, vol. 12, pp. 1658-1661, 2013, doi: 10.1109/LAWP.2013.2294751.

[2] S. -W. Qu, J. -L. Li, Q. Xue and C. -H. Chan, "Wideband Periodic Endfire Antenna With Bowtie Dipoles," in *IEEE Antennas and Wireless Propagation Letters*, vol. 7, pp. 314-317, 2008, doi: 10.1109/LAWP.2008.921345.

[3] A. Azari, A. K. Skrivervik and H. Aliakbarian, "Design Methodology for Wideband Bowtie Patch Antenna for 5G mmWave Applications," *2023 17th European Conference on Antennas and Propagation (EuCAP)*, Florence, Italy, 2023, pp. 1-4, doi: 10.23919/EuCAP57121.2023.10132909.

[4] P. Priyalatha, P. Choudhary and R. Kumari, "Ultra-Wideband Edge Trimmed Bowtie Antenna for X-band Radar Communication," *2023 IEEE 13th Annual Computing and Communication Workshop and Conference (CCWC)*, Las Vegas, NV, USA, 2023, pp. 1231-1235, doi: 10.1109/CCWC57344.2023.10099062.

[5] T. S. Teeslink, D. Torres, J. L. Ebel, N. Sepulveda and D. E. Anagnostou, "Reconfigurable Bowtie Antenna Using Metal-Insulator Transition in Vanadium Dioxide," in *IEEE Antennas and Wireless Propagation Letters*, vol. 14, pp. 1381-1384, 2015, doi: 10.1109/LAWP.2015.2407858.

[6] A. Mansoul, "Reconfigurable multiband bowtie antenna for WiFi, WiMax, and WLAN applications," *2017 IEEE International Symposium on Antennas and Propagation & USNC/URSI National Radio Science Meeting*, San Diego, CA, USA, 2017, pp. 1147-1148, doi: 10.1109/APUSNCURSINRSM.2017.8072616.

[7] P. Rawal and S. Rawat, "A Bowtie Shaped Frequency Reconfigurable Microstrip Patch Antenna with Wide Coverage Area," *2020 5th IEEE International Conference on Recent Advances and Innovations in Engineering (ICRAIE)*, Jaipur, India, 2020, pp. 1-4, doi: 10.1109/ICRAIE51050.2020.9358341.

[8] R. Allanic *et al.*, "Three-State Microwave Tunable Resonator Integrating Several Active Elements on Silicon Technology in a Global Design," in *IEEE Microwave and Wireless Components Letters*, vol. 28, no. 2, pp. 141-143, 2018.

[9] T. Karacolak, *et al.,* "Silicon Carbide (SiC) Antennas for High-Temperature and High-Power Applications," in *IEEE Antennas and Wireless Propagation Letters*, vol. 12, 2013.

[10] The National mmWave Measurement Laboratory. [Online]. Available: https://mmwave.group.shef.ac.uk/.